THE LUNAR SOUTH POLE: A GEOLOGICAL MAP OF THE SOUTH POLE-AITKEN BASIN REGION.

C. M. Poehler[1], C. H. van der Bogert[1], H. Hiesinger[1], M. Ivanov[2] and J.W. Head[3], [1]Institut für Planetologie, Westfälische Wilhelms-Universität, Wilhelm-Klemm-Str. 10, 48149, Münster, Germany, c.poehler@uni-muenster.de, [2]Vernadsky Inst., RAS, Russia, [3]Department of Earth, Environmental and Planetary Sciences, Brown University, Providence, RI 02912 USA.

Introduction: The lunar South Pole is becoming a place of high interest as a destination for robotic and human missions [e.g. 1–4]. This makes detailed studies of the geological background and setting of the region a high priority. Situated on the edge of the South Pole Aitken (SPA) basin, the lunar South Pole poses some observational problems, mainly the presence of large shadows. The entire region is widely influenced by secondaries of the young Orientale basin [5].

Here, we present a geologic map of the lunar South Pole region (***Fig. 1***). The map is part of a complete map of the SPA basin which covers the full extent of the SPA basin, and extends eastward to include part of the Orientale basin.

Methods: The basemap of this map is the Lunar Reconnaissance Orbiter (LRO) Wide-Angle Camera (WAC) (100 m/pixel). For more detailed studies of smaller areas, and for identifying specific features, we used Narrow-Angle Camera (NAC; 0.5 m/pixel) [6] and Kaguya (10 m/pixel) data with different incidence angles. Furthermore, we also used a hybrid spectral mapping technique using Clementine [7], M^3 [8] and Kaguya MI [9] data. We used Lunar Orbiter Laser Altimeter (LOLA) digital elevation models (DEMs) and a LOLA/Kaguya merged DEM with a resolution of 59 m/pixel [10] to identify topographic features. To reduce shadows, particularly in the polar region, we produced hillshade maps with various illumination conditions. We used PLANMAP mapping standards [11],which are an extension of USGS standards [12].

We used morphological appearance and albedo contrast to identify units and determined their relative ages by relationships of embayment and cross-cutting. In addition to relative dating of the units, we performed crater size-frequency distribution (CSFD) measurements and determined absolute model ages (AMAs) using the production and chronology functions of [13]. CSFD measurements were made using CraterTools [14] in ArcGIS, and we determined AMAs with Craterstats [15]. Detailed descriptions of the CSFD measurement technique are given by [16].

Geology: In our study area we defined three classes of geologic features: Basin materials, crater materials, and plains-forming materials.

Basin materials include materials related to the formation of the large basins in the area with the oldest and most dominant being the SPA. We distinguish materials related to the largest basins in the area.

Crater materials are divided into different classes according to the state of degradation and morphology of the craters.

Plains-forming materials summarize relatively flat, smooth surfaces that can be further divided into dark and light plains based on their albedo and iron contents. Most of these plains were also dated to determine their absolute ages.

The materials making up the lunar South Pole region are on top of the southernmost rim of the SPA basin. SPA's rim is obscured by various later impacts and is degraded due to its old age. We were able to find traces of the outer massif, but most of the inner massif is hidden below younger craters and their deposits. Shackleton crater, located almost directly at the South Pole, shows a relatively sharp crater rim, but displays neither extensive ejecta nor rays. We thus interpret it to be Imbrian in age, consistent with other studies [e.g., 18]. The age of Shackleton has significant implications for its likelihood to have accumulated ice. The whole region was influenced by ejecta from the Orientale basin that form crater chains and sharp rim craters oriented toward the basin.

Acknowledgments: This Paper is part of a project that has received funding from the European Union's Horizon 2020 research and innovation program under grant agreement N°776276 (PLANMAP).

References: [1] Flahaut et al. (2020) *PSS 180*. [2] Steenstraet al. (2016) *Adv. Space Res. 58*, 1050–1065. [3] Allender et al. (2018) *Adv. Space Res. 63*, 692–727. [4] Hiesinger et al. (2019) *LPSC 50*, 1327. [5] Stuart-Alexander (1978) *USGS Map I-1047*. [6] Robinson et al. (2010) *Space Sci. Rev., 150*, 81–124. [7] Pieters et al. (1994). *Science, 266*, 1844–1848. [8] Isaacsom et al. (2013). *JGR, 118*, 369–381. [9] Ohtake et al (2013*) Icarus, 226*, 364–374. [10] Barker et al. (2016) *Icarus 273*, 346-355. [11] wiki.planmap.eu/display/public/D2.1-public. [12] FGDC (2006). FGDC-STD-013-2016. [13] Neukum et al. (2001) *Space Sci. Rev. 96*, 55–86. [14] Kneissl et al. (2011) *PSS, 59*, 1243–1254. [15] Michael and Neukum (2010) *EPSL, 294*, 223–229. [16] Hiesinger et al. (2000) *JGR, 105*, 29239–29276. [17] Zuber et al. (2012*) Nature 486*, 378-381.

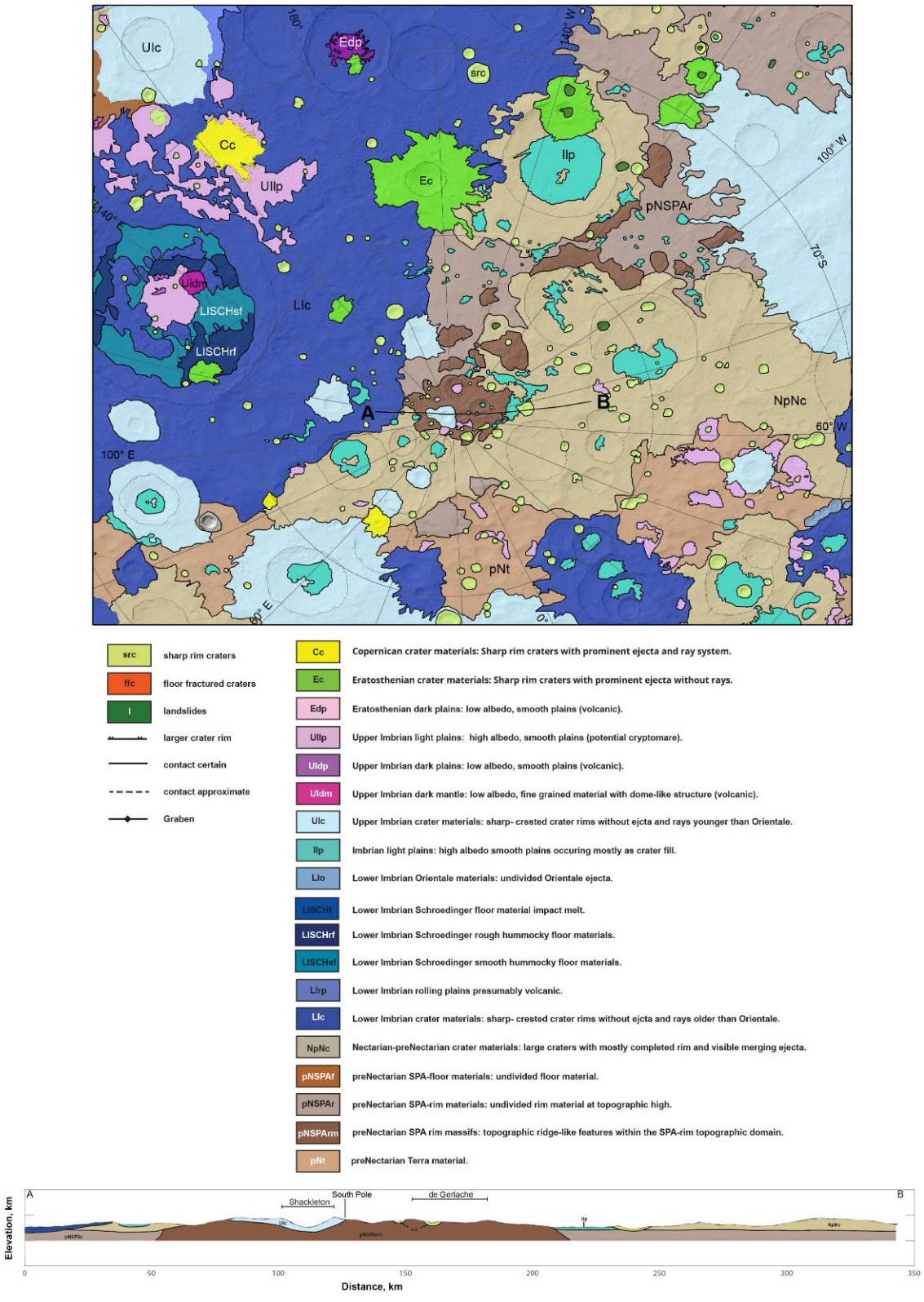

Figure 1. Top: Preliminary geological map of the Lunar South Pole at a scale of 1:500,000 in Lambert projection.. The background image is a hillshade compiled from a LROC LOLA global DEM. –Bottom: Profile across the South Pole.